eLIFE
elifesciences.org

Figures and figure supplements

FRET-based reporters for the direct visualization of abscisic acid concentration changes and distribution in Arabidopsis

Rainer Waadt, et al.

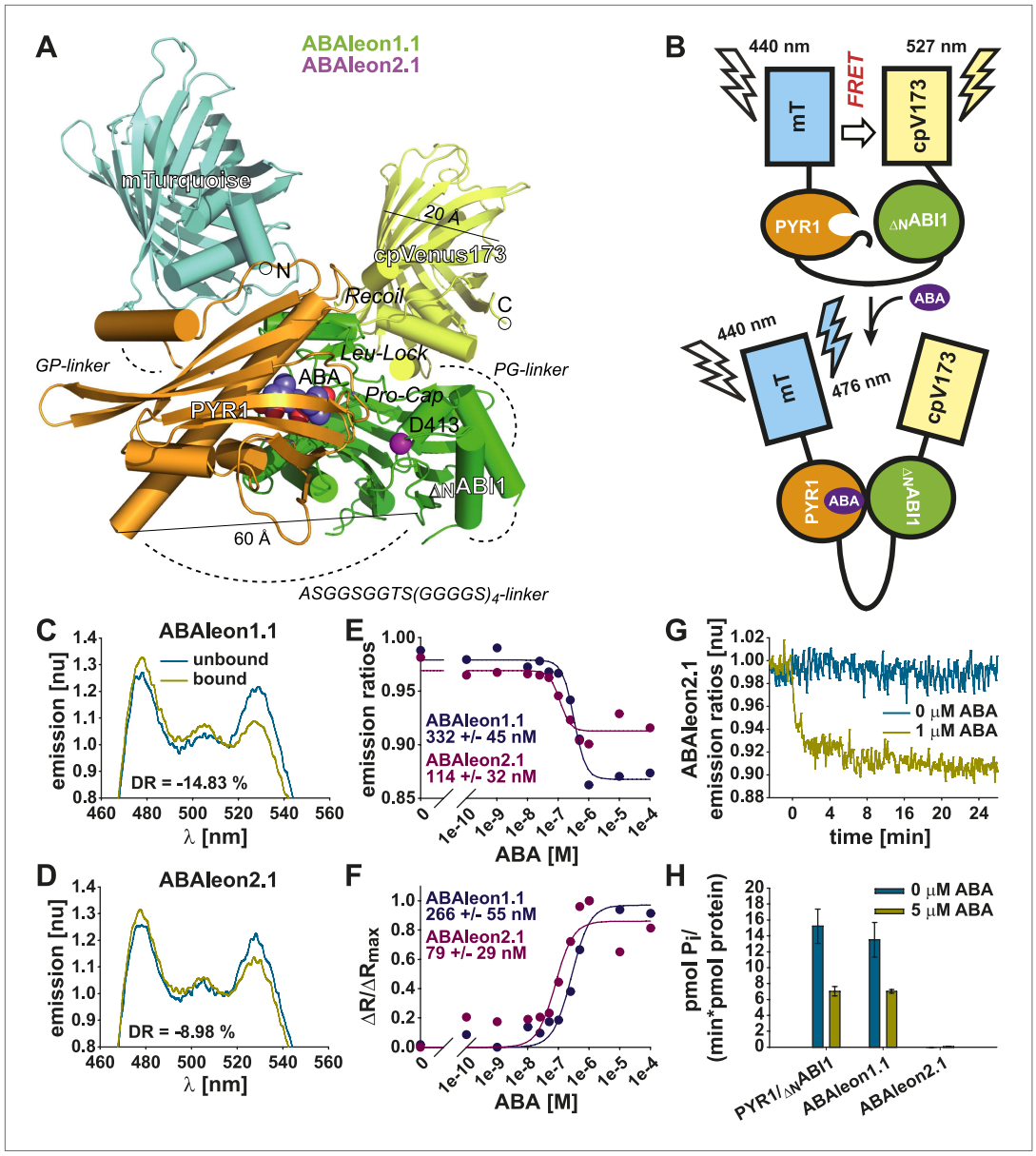

Figure 1. *In vitro* characterization of ABAleons. (**A**) mTurquoise (cyan) is fused through a GP-linker to PYR1 (gold), which is separated by a flexible ASGGSGGTS(GGGGS)$_4$ linker from $_{\Delta N}$ABI1 (green) fused to cpVenus173 (yellow) through a PG linker. Structural features of the PYR1-$_{\Delta N}$ABI1 complex including ABA (blue and red balls), ABI1 D413 (purple ball) and loops controlling access to the ABA binding site are highlighted. Dashed lines indicate linkers and unresolved structures. (**B**) Without ABA, ABAleon flexibility enables FRET from mTurquoise (mT) to cpVenus173 (cpV173). ABA triggered PYR1-$_{\Delta N}$ABI1 binding increases the distance or orientation between the fluorescent probes, thereby reducing FRET efficiency. (**C** and **D**) Normalized (nu) emission spectra of (**C**) ABAleon1.1 and (**D**) ABAleon2.1 in absence (unbound) and in presence (bound) of ABA with indicated dynamic range (DR). (**E**) Emission ratios and (**F**) $\Delta R/\Delta R_{max}$ plotted against increasing [ABA], with indicated ABA affinity K'_d of each ABAleon calculated from the respective plot. (**G**) Time-dependent normalized emission ratios of ABAleon2.1 in response to 0 and 1 μM ABA. (**H**) Phosphatase activity assays of equimolar PYR1 and $_{\Delta N}$ABI1 combinations and indicated ABAleons in presence of 0 and 5 μM ABA (mean ± SD, n = 4).

DOI: 10.7554/eLife.01739.003

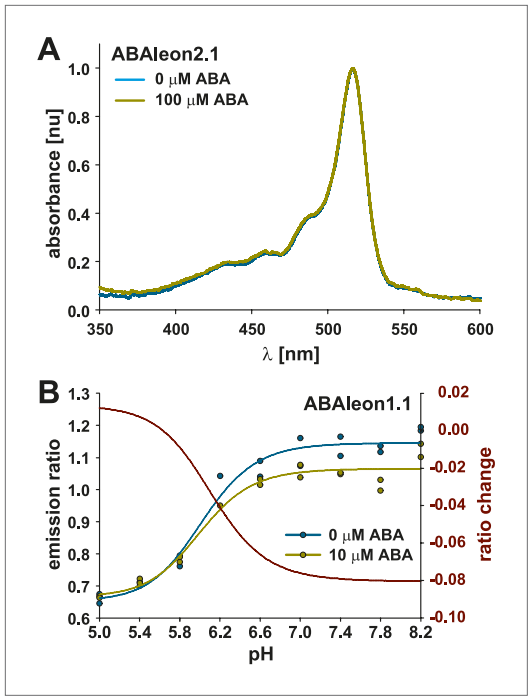

Figure 1—figure supplement 1. ABA does not affect ABAleon absorbance and ABAleon emission is stable at physiological pH conditions.

DOI: 10.7554/eLife.01739.004

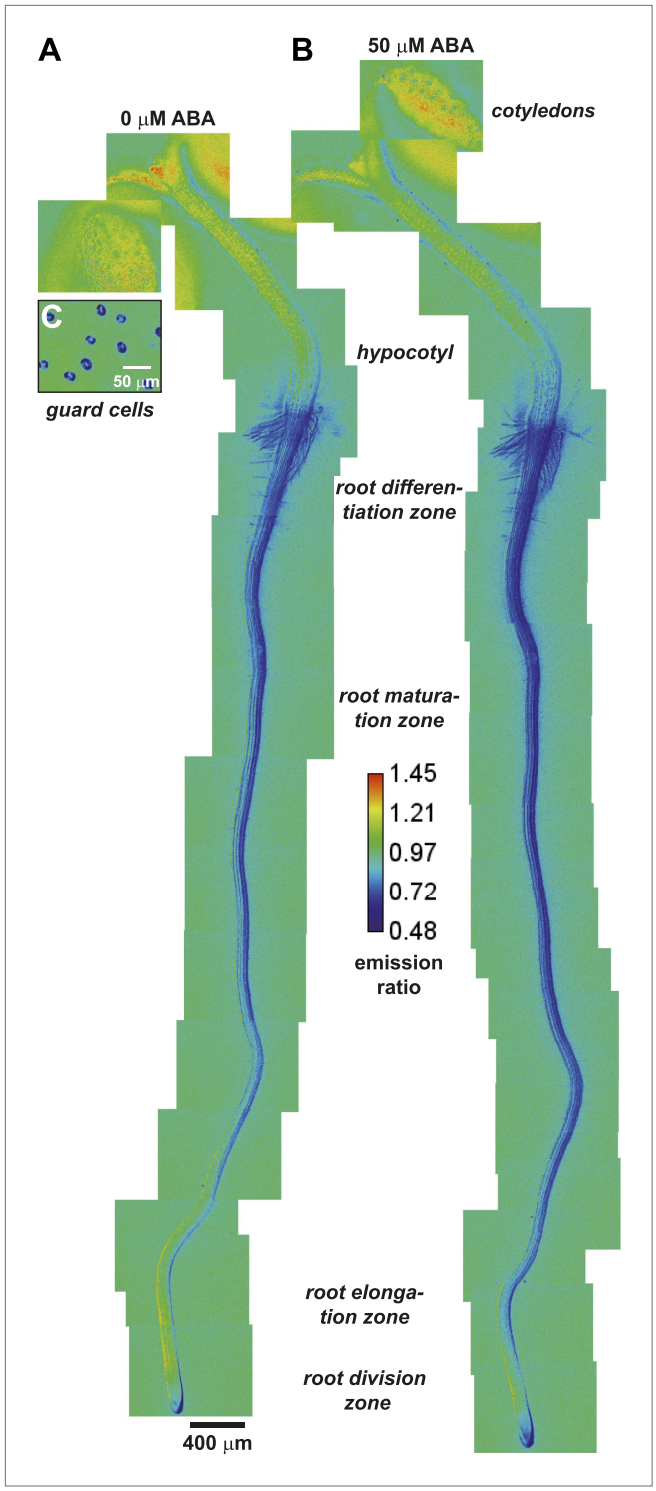

Figure 2. ABA-induced ABAleon2.1 responses in whole seedlings. (**A** and **B**) Manually assembled ABAleon2.1 ratio images (**A**) before and (**B**) 2 h after application of 50 μM ABA. (**C**) Ratio image of untreated guard cells from lower epidermis of 33-day-old soil grown plants. Images were calibrated to the indicated calibration bar. Blue colors indicate low ABAleon2.1 emission ratios, corresponding to high ABA concentrations, and red colors indicate high ABAleon2.1 emission ratios corresponding to low ABA concentrations. Shown is a representative of four experiments.
DOI: 10.7554/eLife.01739.005

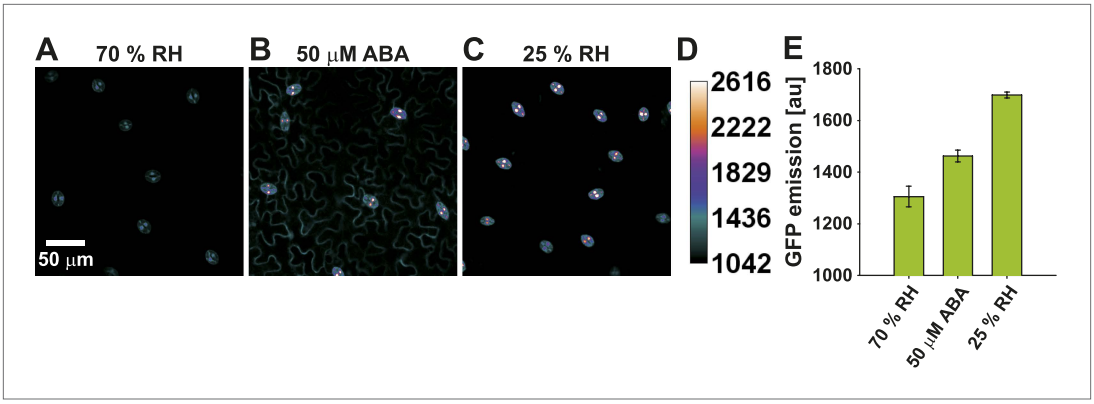

Figure 2—figure supplement 1. pRAB18-GFP expression in guard cells.

DOI: 10.7554/eLife.01739.006

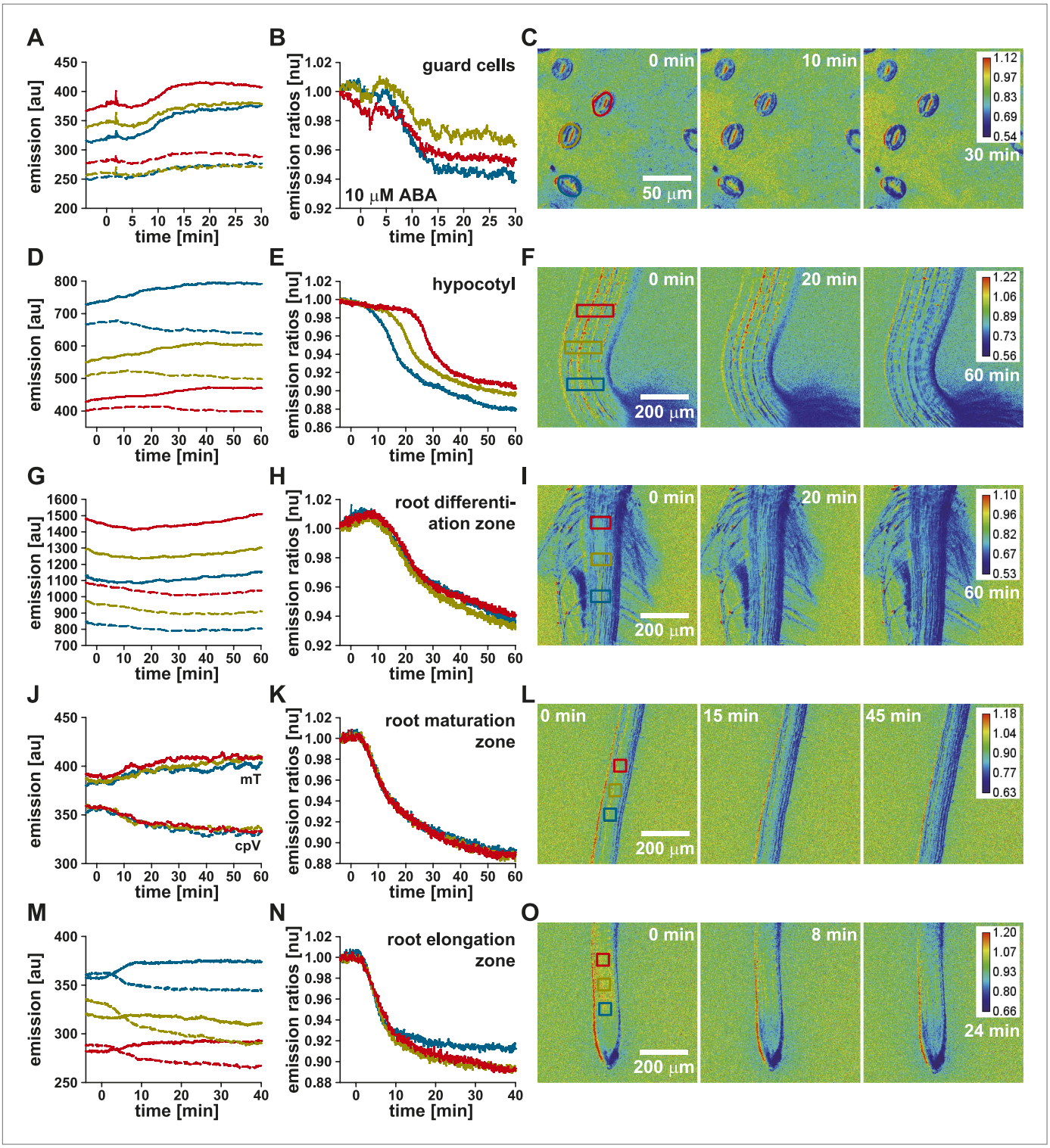

Figure 3. ABA-induced ABAleon2.1 responses in Arabidopsis tissues. Time-resolved ABAleon2.1 responses to 10 µM ABA in (**A**–**C**) guard cells of 45-day-old plants and (**D**–**F**) the hypocotyl, (**G**–**I**) the root differentiation-, (**J**–**L**) maturation- and (**M**–**O**) elongation-zone of 5-day-old seedlings. (**A**, **D**, **G**, **J**, **M**) Time course of mTurquoise (mT, solid lines) and cpVenus173 emission (cpV, dashed lines) and (**B**, **E**, **H**, **K**, **N**) the corresponding normalized emission ratios colored according to the analyzed regions boxed in the in initial t = 0 min images (**C**, **F**, **I**, **L**, **O**). Each analysis is a representative of 3–4 experiments. Note, that there is a slight sample drift, which causes cpVenus173 emission increases in (**A**).

DOI: 10.7554/eLife.01739.007

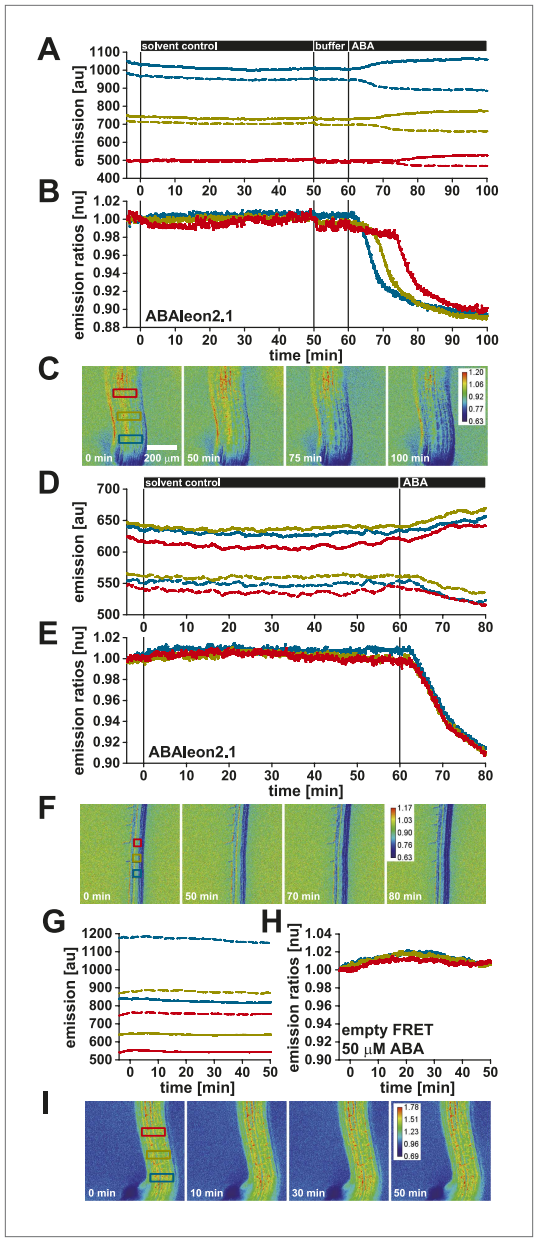

Figure 3—figure supplement 1. ABAleon2.1 but not the empty FRET cassette responds specifically to ABA.

DOI: 10.7554/eLife.01739.008

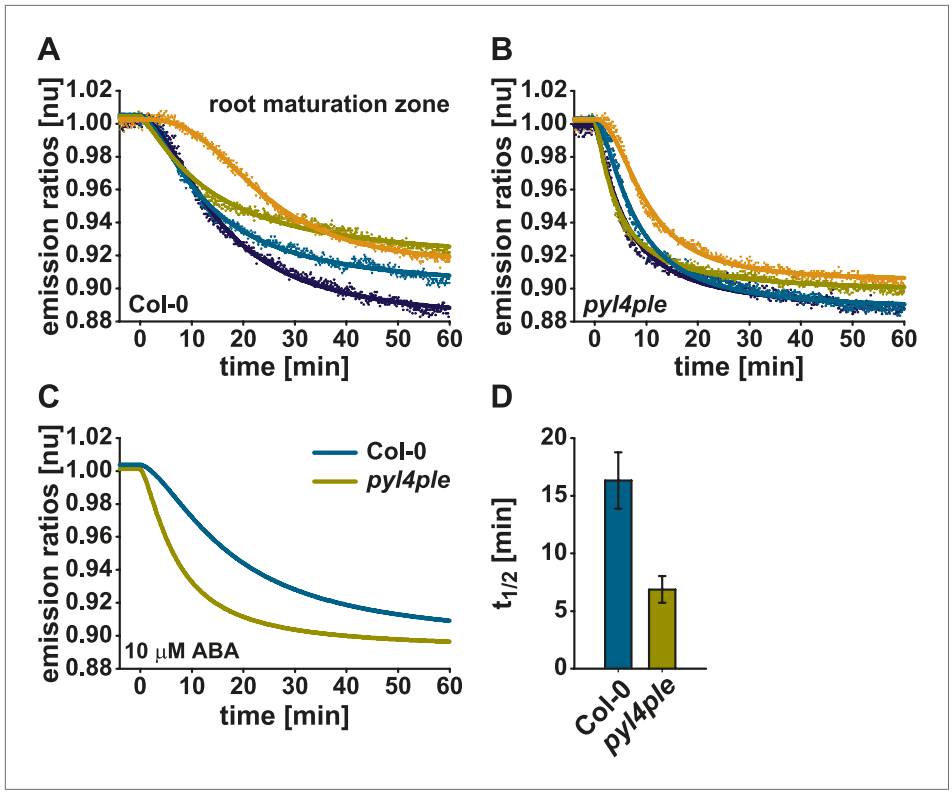

Figure 4. Accelerated ABAleon2.1 responses in roots of the *pyl4ple* mutant. Normalized 10 µM ABA-induced ABAleon2.1 emission ratio changes in the root maturation zone of Col-0 (**A**, **C** cyan line) and *pyr1-1/pyl1-1/pyl2-1/pyl4-1* (*pyl4ple*) (**B**, **C** yellow line). (**A** and **B**) Data points from single measurements fitted by the respective four parameter logistic curve. (**C**) Combined data from four experiments in (**A** and **B**) fitted by the respective four parameter logistic curve. (**D**) $t_{1/2}$ values (means ± SEM, n = 4) calculated from the fitted curves in (**A** and **B**).
DOI: 10.7554/eLife.01739.010

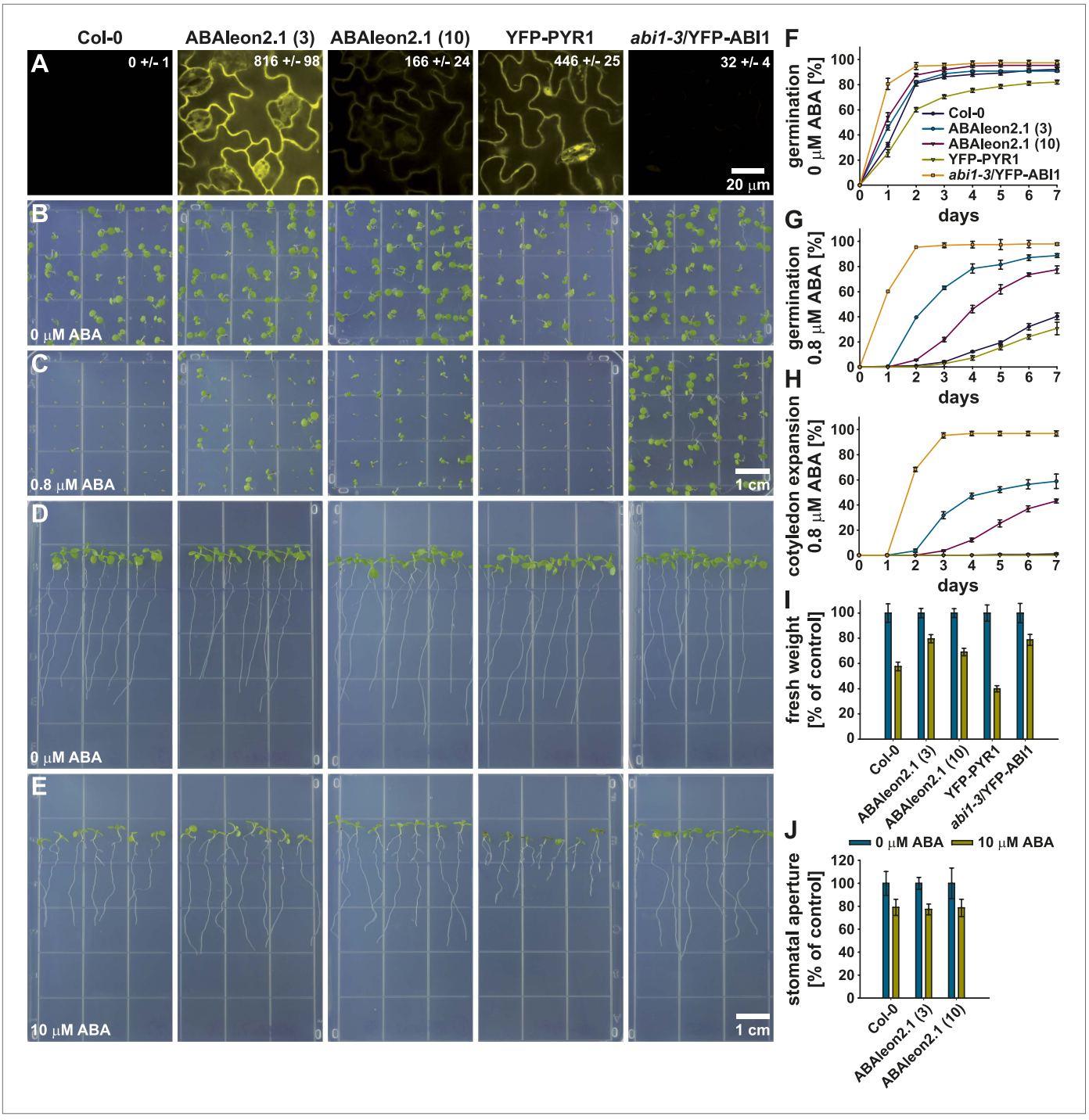

Figure 5. ABAleon2.1-expressing plants show an ABA hyposensitivity. From left to right, Col-0 wild type, ABAleon2.1 (line 3), ABAleon2.1 (line 10), YFP-PYR1 and *abi1-3*/YFP-ABI1. (**A**) Analyses of cpVenus173/YFP fluorescence emission in the leaf epidermis. Numerical fluorescence intensity values in the images represent means ± SEM of n = 4 images. (**B** and **C**) 7-day-old seedlings germinated and grown on 0.5 MS media supplemented with (**B**) 0 and (**C**) 0.8 μM ABA. (**D** and **E**) 9-day-old seedlings 5 days after transfer to 0.5 MS media supplemented with (**D**) 0 and (**E**) 10 μM ABA. (**F**–**H**) 7 day time course of (**F** and **G**) seed germination and (**H**) cotyledon expansion in presence of (**F**) 0 and (**G** and **H**) 0.8 μM ABA normalized to the seed count of each replicate (means ± SEM, n = 4 technical replicates with 49 seeds/n). (**I**) Fresh weight of seedlings from (**D** and **E**) normalized to the 0 μM ABA control conditions (means ± SEM, n = 5 technical replicates with seven seedlings/n). (**J**) Stomatal aperture of 20-23-day old seedlings exposed to 10 μM ABA normalized to the 0 μM ABA control conditions (means ± SEM, n = 3 with ≥ 24 stomata/n).

DOI: 10.7554/eLife.01739.011

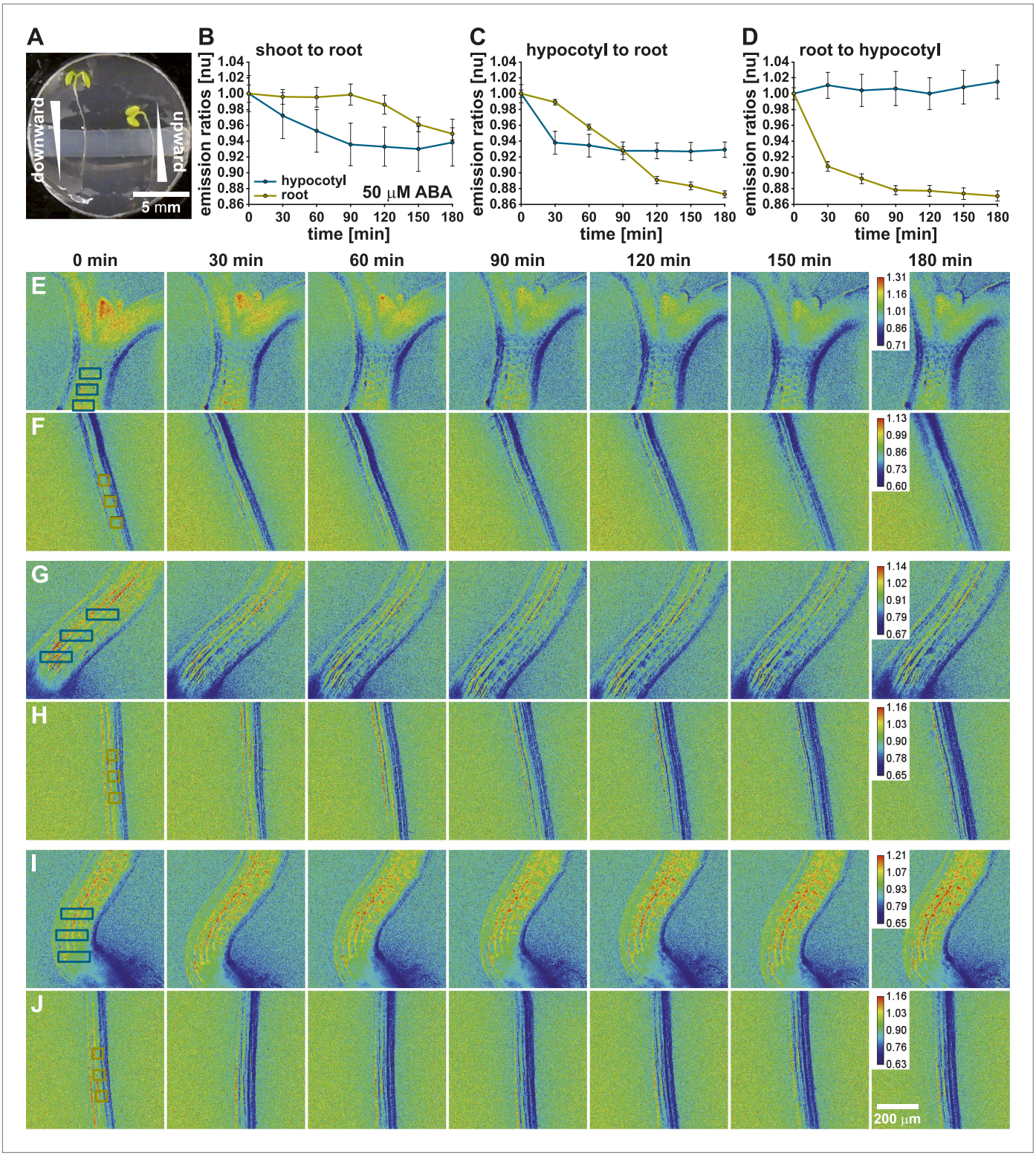

Figure 6. Visualization of long-distance ABA transport. (**A**) ABAleon2.1 seedlings were transferred to microscope dishes, which were divided into two isolated experimental chambers by a horizontal block of modeling clay. (**B**, **E**, **F**) Shoot-to-root, (**C**, **G**, **H**) hypocotyl-to-root and (**D**, **I**, **J**) root-to-hypocotyl ABA transport after application of 50 µM ABA. (**B**–**D**) Time-dependent normalized emission ratios (means ± SEM, n = 3) in the hypocotyl (cyan) and root (yellow) were quantified in three regions indicated by boxes in the initial images (**E**–**J**). The calibration bar in the final t = 180 min image indicates the scale of the emission ratios. Decreasing ratios indicate ABA accumulation. Shown are representative analyses of 3–4 experiments.

DOI: 10.7554/eLife.01739.012

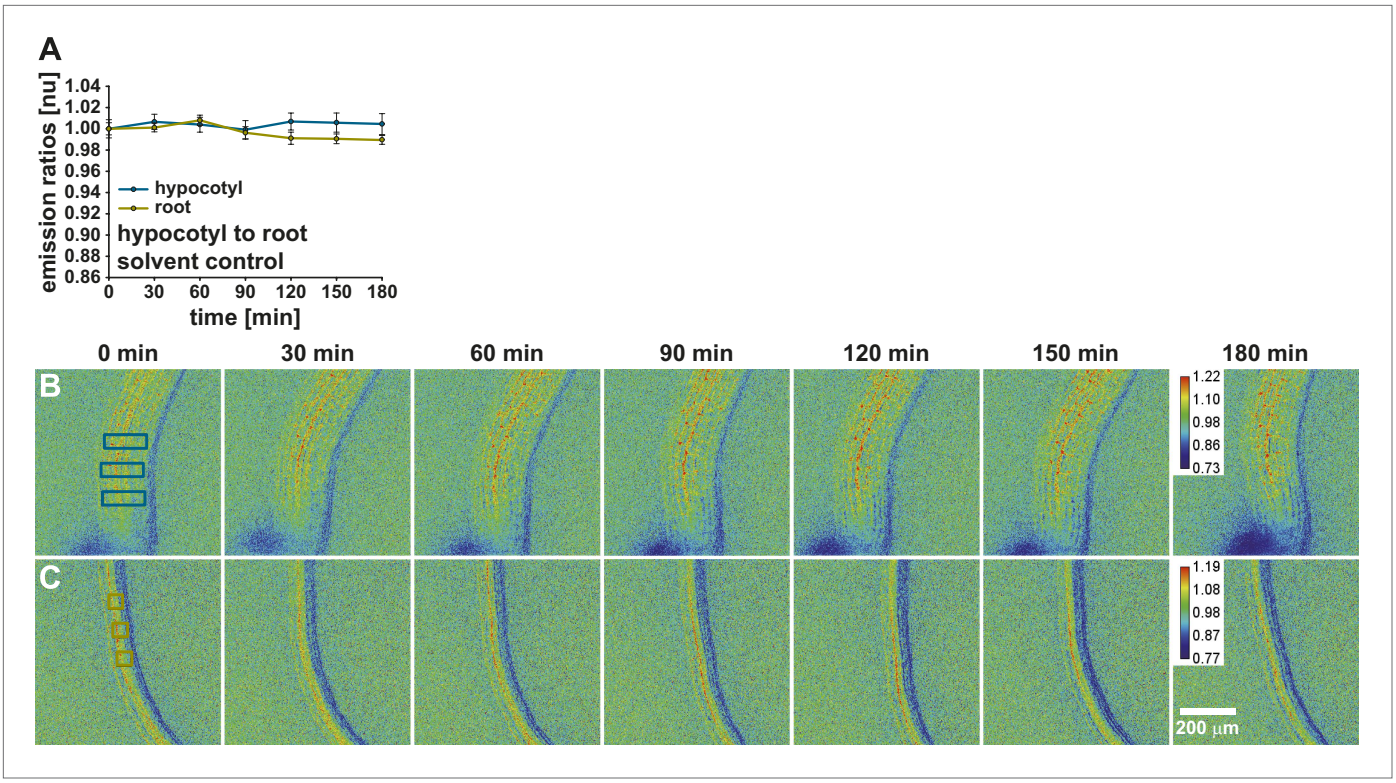

Figure 6—figure supplement 1. Solvent control for long-distance ABA transport.

DOI: 10.7554/eLife.01739.013

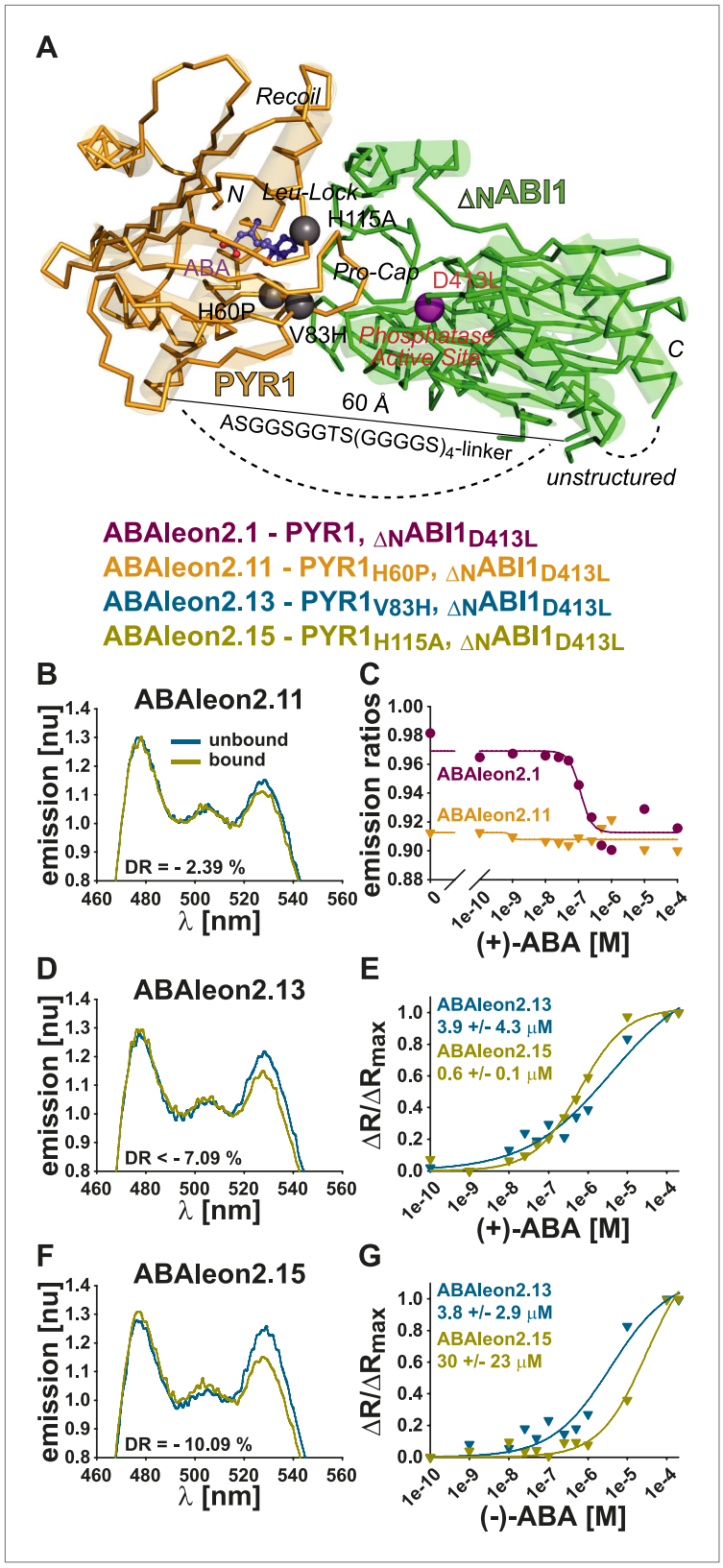

Figure 7. *In vitro* analyses of ABAleon2.1 mutants. (**A**) Structural model of the PYR1(gold)-ABA(purple)-ABI1(green) complex, indicating mutations in ABAleon2.1 that were analyzed in (**B**–**G**): H60P monomer-inducing, V83H in Pro-Cap and H115A in Leu-Lock of PYR1 (grey balls) and D413L phosphatase-inactivating in ABI1 (purple ball). Emission spectra

Figure 7. Continued on next page

Figure 7. Continued

of (**B**) ABAleon2.11, (**D**) ABAleon2.13 and (**F**) ABAleon2.15 in the absence (unbound) and presence of (+)-ABA (bound) with indicated dynamic range (DR). (**B**) ABAleon2.11 exhibited no clear response to ABA. (**C**) (+)-ABA titrations of ABAleon2.11 compared to ABAleon2.1 suggest saturation of ABAleon2.11 in the absence of ABA. (**E** and **G**) $\Delta R/\Delta R_{max}$ plots of ABAleon titrations with (**E**) naturally occurring (+)-ABA and (**G**) its enantiomer (−)-ABA, which binds more weakly. The respective apparent ABA affinities (K'_d) are indicated.

DOI: 10.7554/eLife.01739.014

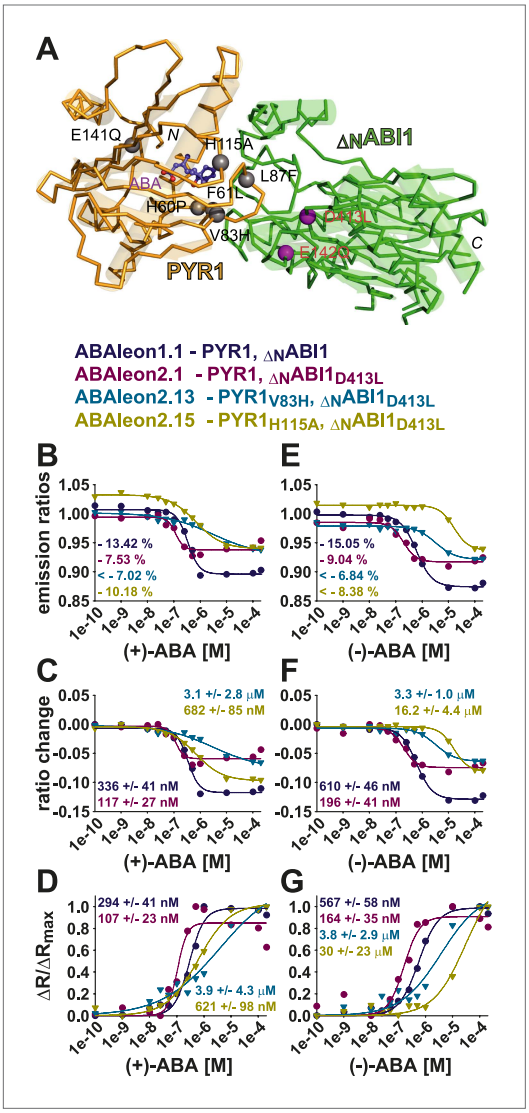

Figure 7—figure supplement 1. (+)- and (−)-ABA titrations of selected ABAleons.

DOI: 10.7554/eLife.01739.015

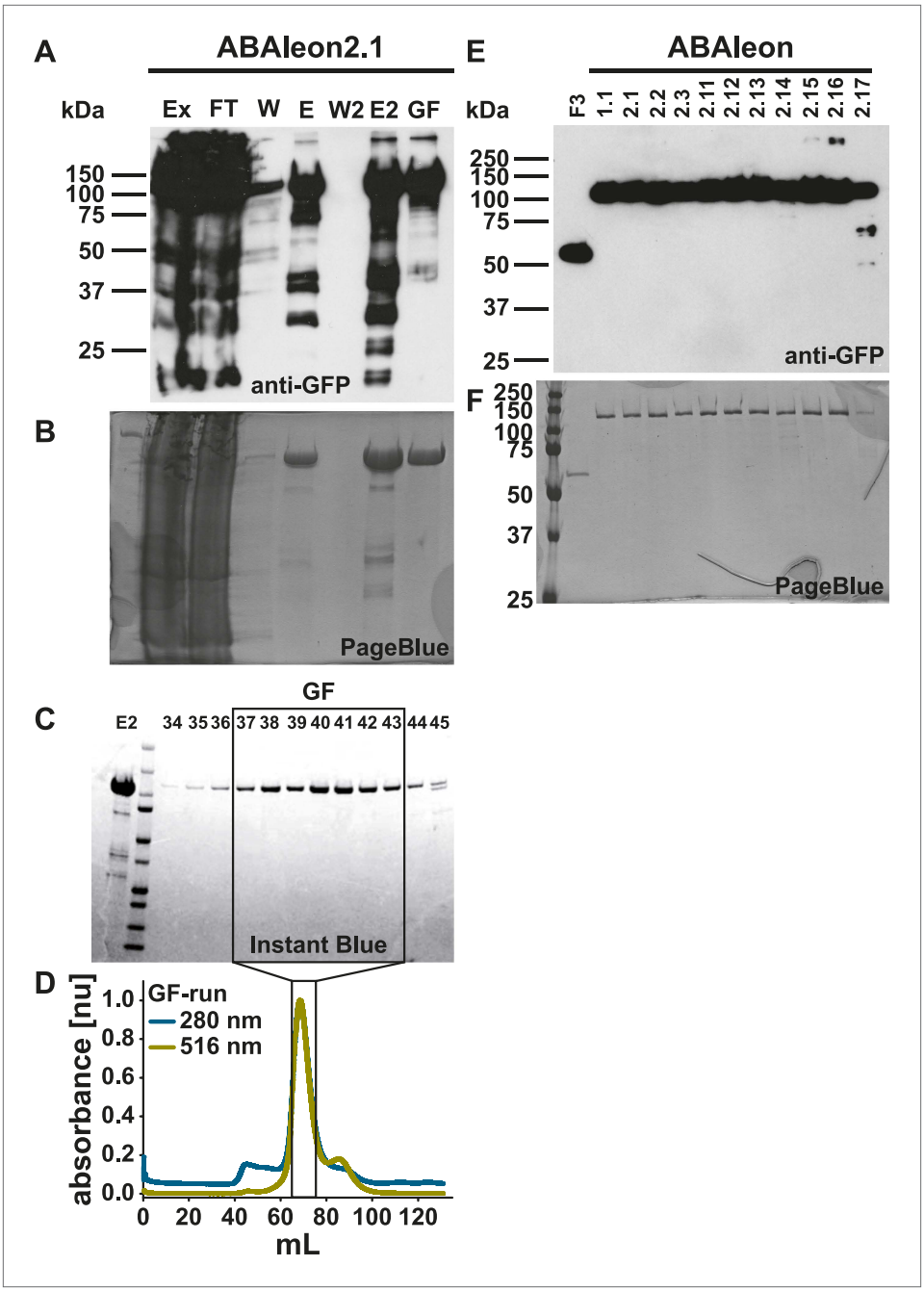

Figure 7—figure supplement 2. Purification of ABAleons after expression in *E. coli*.
DOI: 10.7554/eLife.01739.016

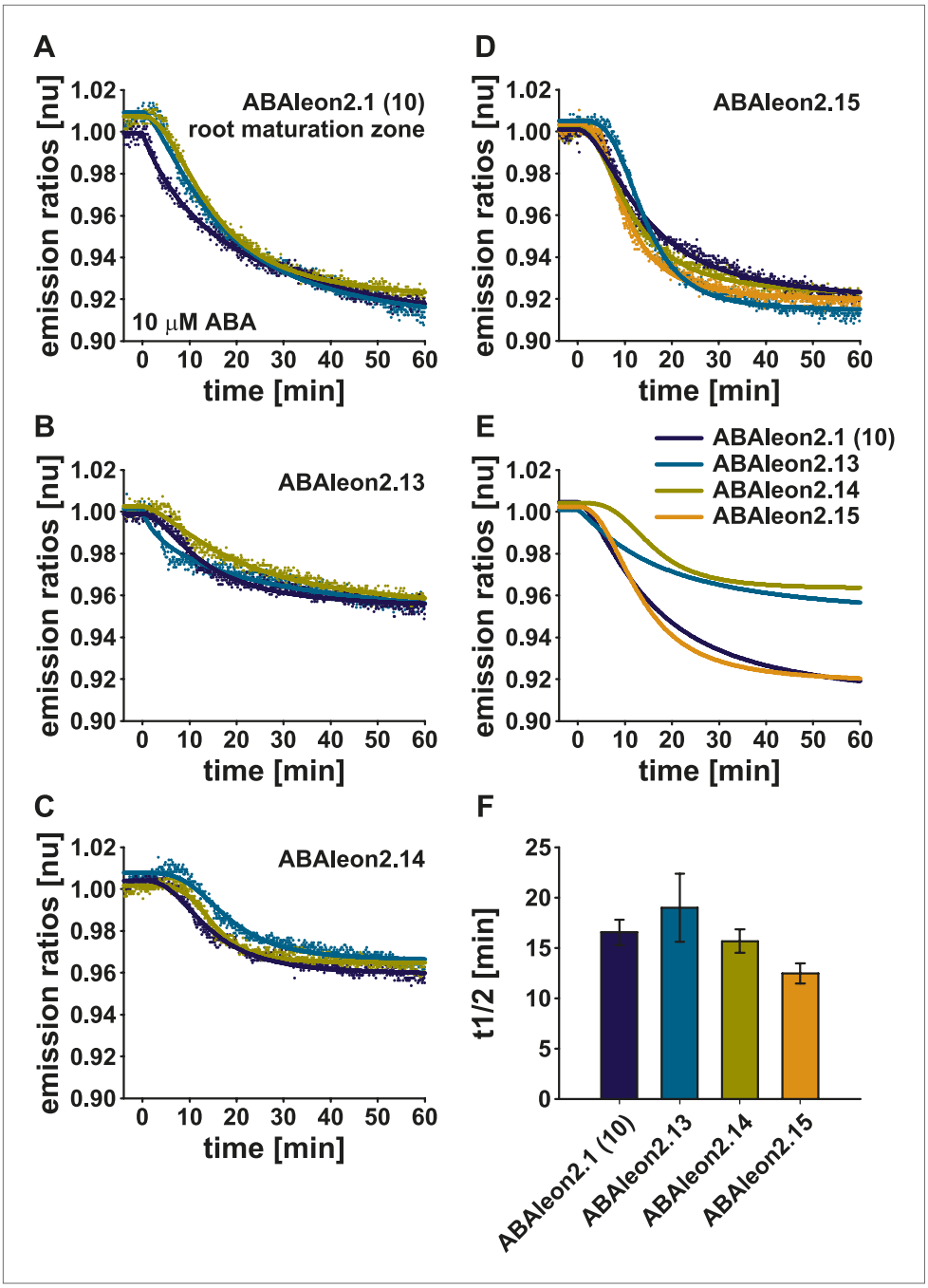

Figure 8. ABA-induced ABAleon2.1 (line 10), ABAleon2.13, ABAleon2.14 and ABAleon2.15 responses in the root maturation zone. 10 μM ABA-induced normalized emission ratio changes in the root maturation zone of (**A**, **E** dark blue line) ABAleon2.1 (line 10), (**B**, **E** cyan line) ABAleon2.13, (**C**, **E** yellow line) ABAleon2.14, and (**D**, **E** orange line) ABAleon2.15. (**A**–**D**) Data points from single measurements fitted by the respective four parameter logistic curve. (**E**) Combined data from three to four experiments in (**A**–**D**) fitted by the respective four parameter logistic curve. (**F**) $t_{1/2}$ values (means ± SEM, n = 3–4) calculated from the fitted curves in (**A**–**D**).

DOI: 10.7554/eLife.01739.018

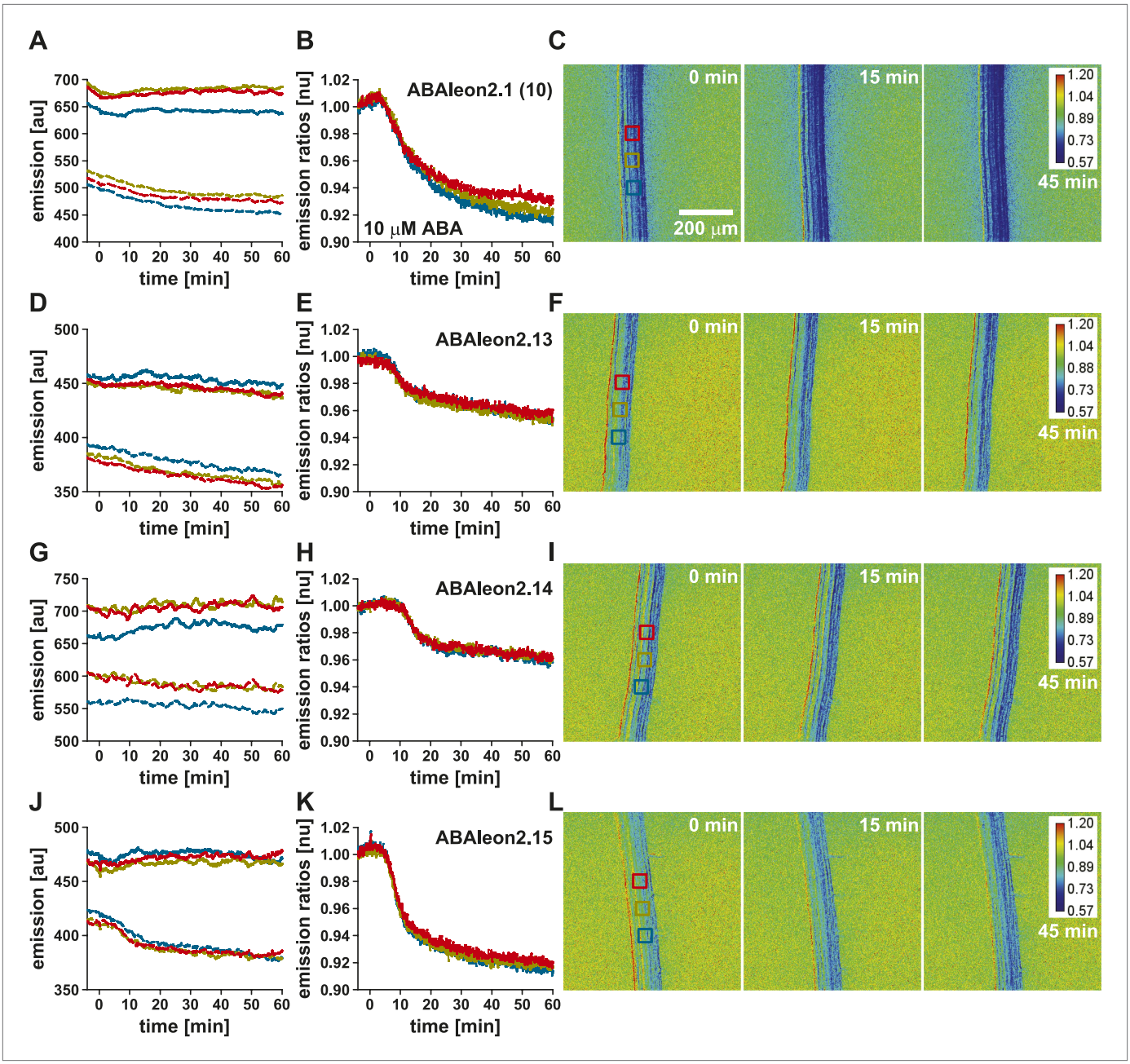

Figure 8—figure supplement 1. ABA-induced ABAleon2.1 (line 10), ABAleon2.13, ABAleon2.14 and ABAleon2.15 responses in the root maturation zone (examples).

DOI: 10.7554/eLife.01739.019

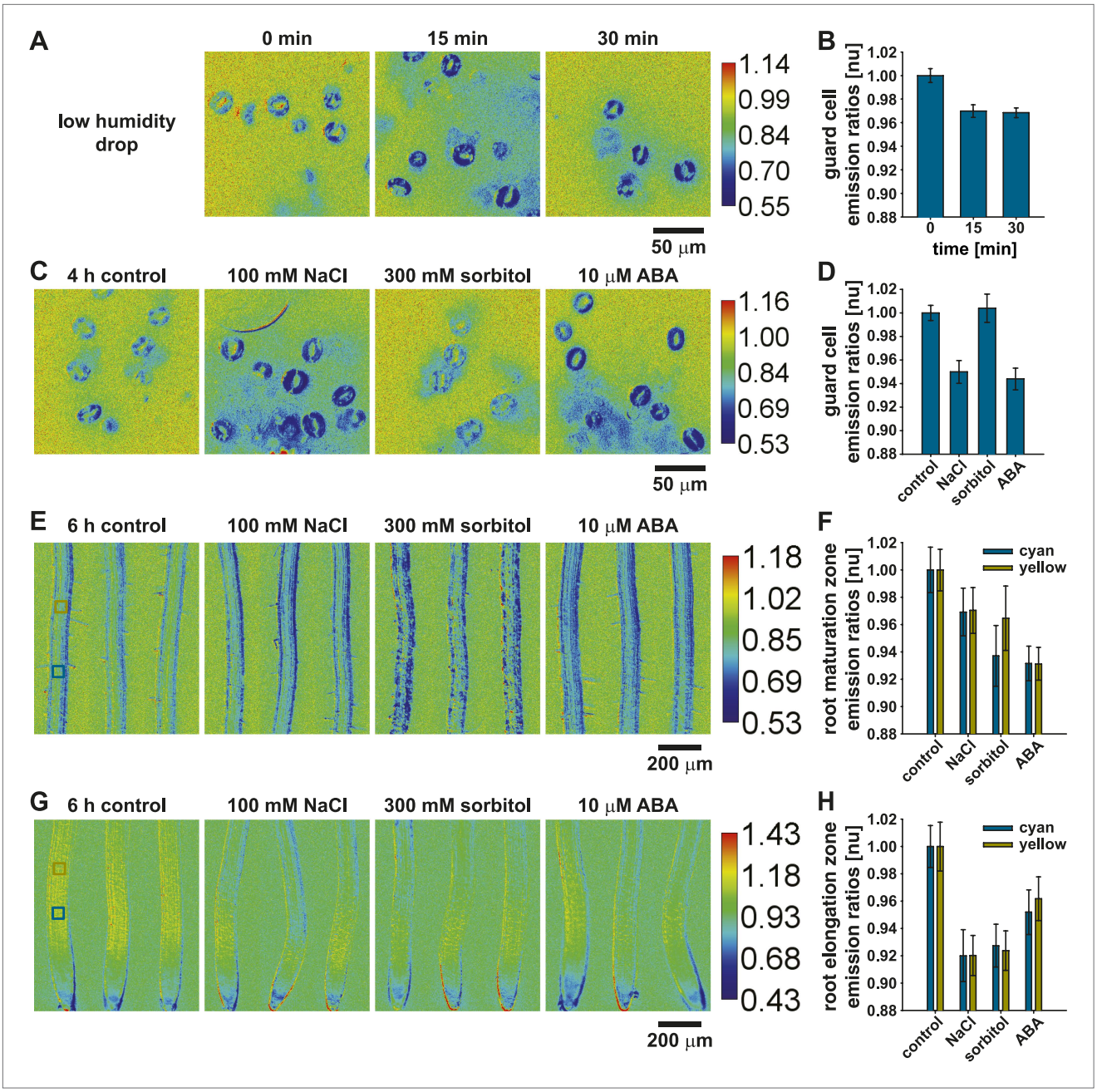

Figure 9. ABAleon2.1 reports ABA concentration changes in response to low humidity, salt and osmotic stress. ABAleon2.1 emission ratios in response to (**A** and **B**) low humidity and (**C**–**H**) 4–6 h treatments with 0.01 % EtOH (control), 100 mM NaCl, 300 mM sorbitol and 10 μM ABA in (**C** and **D**) guard cells, (**E** and **F**) the root maturation- and (**G** and **H**) elongation zone. (**A**, **C**, **E**, **G**) Representative emission ratio images with indicated calibration bars. (**B** and **D**) Normalized emission ratios in guard cells (means ± SEM, n = 3 with ≥ 24 guard cell pairs/n). (**F** and **H**) Normalized emission ratios analyzed from two boxed regions (cyan and yellow) color-coded in the left images of (**E** and **G**) (means ± SEM, n = 8–10 seedlings).

DOI: 10.7554/eLife.01739.020